


Lipid peroxidation increases hydrogen peroxide permeability leading to cell death in cancer cell lines that lack mtDNA

Kazuo Tomita¹  | Yuko Takashi^{1,2} | Yuya Ouchi³ | Yoshikazu Kuwahara^{1,4} | Kento Igarashi¹ | Taisuke Nagasawa¹ | Hideki Nabika³ | Akihiro Kurimasa⁴ | Manabu Fukumoto⁵ | Yoshihiro Nishitani² | Tomoaki Sato¹

¹Department of Applied Pharmacology, Graduate School of Medical and Dental Sciences, Kagoshima University, Kagoshima, Japan

²Department of Restorative Dentistry and Endodontology, Graduate School of Medical and Dental Sciences, Kagoshima University, Kagoshima, Japan

³Department of Material and Biological Chemistry, Faculty of Science, Yamagata University, Yamagata, Japan

⁴Department of Radiation Biology and Medicine, Faculty of Medicine, Tohoku Medical and Pharmaceutical University, Sendai, Japan

⁵Department of Molecular Pathology, Tokyo Medical University, Tokyo, Japan

Correspondence

Kazuo Tomita, Department of Applied Pharmacology, Graduate School of Medical and Dental Sciences, Kagoshima University, 8-35-1 Sakuragaoka, Kagoshima 890-8544, Japan.
Email: ktomita@dent.kagoshima-u.ac.jp

Funding information

JSPS KAKENHI, Grant/Award Number: 16K00538 and 16K11513; Kodama Memorial Fund for Medical Research, Grant/Award Number: 265

Abstract

4-Hydroxynonenal (HNE) is an important product of plasma membrane lipid peroxidation, which is a cause of cell and tissue injury. Mitochondrial DNA (mtDNA)-depleted ρ^0 cells were established using human cervical cancer and oral squamous cell carcinoma cell lines. We investigated the effect of reactive oxygen species in ρ^0 cells, especially the mechanism of hydrogen peroxide (H_2O_2)-mediated cell death. These cells were subjected to high oxidative stress and, compared with their parental cells, showed greater sensitivity to H_2O_2 and high lipid peroxidation. Upregulation of HNE in the plasma membrane was observed prior to the increase in intracellular H_2O_2 . The amount of oxidized lipid present changed H_2O_2 permeability and administration of oxidized lipid led to further cell death after treatment with H_2O_2 . Expression levels of lipoxygenase ALOX genes (ie ALOX5, ALOX12, and ALOX15) were upregulated in ρ^0 cells, as were expression levels of ALOX12 and ALOX15 proteins. ALOX5 protein was mainly distributed in the nucleus, while ALOX12 and ALOX15 proteins were distributed in the nucleus and the cytoplasm. Although expression of COX2 gene was upregulated, its protein expression did not increase. ALOX (especially ALOX15) may be involved in the sensitivity of cancer cells to treatment. These data offer promise for the development of novel anticancer agents by altering the oxidation state of the plasma membrane. Our results showed that lipid peroxidation status is important for H_2O_2 sensitivity and that ALOX15 is involved in lipid peroxidation status.

KEYWORDS

cell membrane, hydrogen peroxide, lipid peroxidation, mitochondria, oxidative stress

Abbreviations: •OH, hydroxyl radical; ALOX, lipoxygenase; COX, cyclooxygenase; DOPC, 1,2-dioleoyl-sn-glycero-3-phosphocholine; H_2O_2 , hydrogen peroxide; HNE, 4-Hydroxynonenal; HPF, Hydroxyphenyl fluorescein; MIC, microscope observation; NDGA, nordihydroguaiaretic acid; PINK1, PTEN-induced kinase 1; POVPC, 1-palmitoyl-2-(5'-oxo-valeryl)-sn-glycero-3-phosphocholine; ROS, Reactive oxygen species; RT, radiation therapy.

Tomita and Takashi are contributed equally to this work.

This is an open access article under the terms of the Creative Commons Attribution-NonCommercial License, which permits use, distribution and reproduction in any medium, provided the original work is properly cited and is not used for commercial purposes.

© 2019 The Authors. *Cancer Science* published by John Wiley & Sons Australia, Ltd on behalf of Japanese Cancer Association.

1 | INTRODUCTION

ROS are defined as chemically reactive species containing oxygen, some of which are peroxidases or hydroxyl radicals. ROS production is effective in the chemotherapy and RT of cancer.¹⁻³ Numerous chemicals can produce ROS than affect cancer cells⁴⁻⁸ and some of these are under investigation in clinical trials.⁹ Some ROS, for example H₂O₂, are used as sensitizers of cancer cells by producing reactive oxygen during RT.^{10,11} Similarly, ROS are produced by nicotinamide adenine dinucleotide phosphate (NADPH) oxidase in the cytoplasm.¹² However, the main source of ROS may be the mitochondrial electron transport chain through oxidative phosphorylation.^{13,14} Mitochondrial DNA (mtDNA) encodes 13 proteins that are components of the mitochondrial electron transport chain. Damage to mtDNA results in increased production of ROS, conversely causing neurodegenerative diseases and various types of cancer.^{15,16} Therefore, these mtDNA-damaged cells may be valuable models for studying ROS-related disease. Mitochondrial DNA devoid ρ⁰ cells were established from a human cervical cancer cell line (HeLa) and from an oral squamous cell carcinoma (SAS). These ρ⁰ cells were sensitive to ROS, in particular H₂O₂.¹⁷ Notably, yeast ρ⁰ cells have also shown sensitivity to treatment with H₂O₂.¹⁸ Recently, ρ⁰ cells from osteosarcoma and lung carcinoma have shown sensitivity to X-ray irradiation related to oxidative stress.¹⁹ Conversely, there are several studies reporting that ρ⁰ cells are resistant to oxidative stress, especially to radiation. ρ⁰ cells from human fibroblasts have shown resistance to γ-irradiation by decreasing apoptosis.²⁰ In addition, ρ⁰ cells from the human pancreatic tumor MiaPaCa-2 cell line showed resistance to X-ray irradiation via activation of cyclin B1.²¹ Moreover, ρ⁰ cells from healthy human bronchial epithelial cells have shown resistance to oxidative stress. At present, the sensitivity or resistance of ρ⁰ cells to oxidative stress and the stress response mechanism involved in these processes have not been fully elucidated.

ROS react with polyunsaturated fatty acids in the lipid membranes, inducing lipid peroxidation that leads to cell death. HNE, the end product of lipid peroxidation reacts with low-molecular-weight compounds (eg, glutathione, proteins, and DNA), and is considered a second messenger of oxidative stress.^{22,23} Notably, HNE production occurs through the ROS generation and an enzymatic process.²⁴ The key enzyme in the production of HNE is ALOX15. The relationship between the level of HNE and ALOX15 has been previously reported.²⁵ It has also been reported HNE induces expression of the COX2 gene.²⁶ However, so far, the relationship between ρ⁰ cells and ALOXs and/or COX2 has not been investigated.

Moreover, the mechanism of sensitivity to H₂O₂ in ρ⁰ cells via oxidation of the plasma membrane has not been elucidated. In this study, we investigated the oxidation state of the plasma membrane in ρ⁰ cells, and identified factors that control this process.

2 | MATERIALS AND METHODS

2.1 | Cell culture

Human cancer cell lines HeLa and SAS were obtained from the Cell Resource Center for Biomedical Research, Institute of Development,

Aging and Cancer, Tohoku University (Sendai, Japan). ρ⁰ cells were established through culture in RPMI1640 (Wako Pure Chemical Industries Ltd., Osaka, Japan) containing 5% FBS (Gibco Invitrogen Corp., Carlsbad, CA, USA), 50 ng/mL ethidium bromide (Nacalai Tesque Inc., Kyoto, Japan), 50 μg/mL uridine (Sigma-Aldrich, St Louis, MO, USA), and 110 μg/mL sodium pyruvate (Sigma-Aldrich) for 3-4 wk.¹⁷ Cells were maintained in RPMI 1640 supplemented with 10% FBS, 50 μg/mL uridine, and 110 μg/mL sodium pyruvate in a humidified atmosphere at 37°C with 5% carbon dioxide. Exponentially growing cells were used in all experiments.

2.2 | Relative levels of internal H₂O₂

Internal H₂O₂ was visualized using HYDROP™ (Goryo Chemical Inc., Hokkaido, Japan) as previously described.¹⁷ Briefly, cells in glass-bottomed dishes (Matsunami Glass Ind., Ltd., Osaka, Japan) were cultured in RPMI 1640 with or without 50 μmol/L H₂O₂ for 10 min, 30 min, 1 h, and 2 h. The cultured cells were washed with noncontaining H₂O₂ RPMI 1640 twice to remove the H₂O₂ from the medium, and subjected to treatment with 2.5 μmol/L HYDROP™ in RPMI 1640 at 37°C for 20 min. Subsequently, the cells were washed with RPMI 1640 twice, and fluorescence images were obtained using a BZ-8000 fluorescence microscope (Keyence Corporation, Osaka, Japan). The ImageJ software (Rasband, W.S., ImageJ, U.S. National Institutes of Health, Bethesda, Maryland, USA, <http://rsb.info.nih.gov/ij/>, 1997-2012) was used to measure fluorescence intensity.

2.3 | Intracellular intake of H₂O₂ using a stable isotope

A H₂O₂¹⁸O₂ solution (Sigma-Aldrich) was used to measure the intracellular intake of H₂O₂. Cells were subjected to treatment with 50 μmol/L H₂O₂¹⁸O₂ solution for 1 h. After treatment, the cells were washed with phosphate-buffered saline (PBS) three times. Following the wash, the cells were collected and dried using an FDU-2200 freeze dryer (Tokyo Rikakikai Co. Ltd., Tokyo, Japan) for 3 h. Dried samples were sent for analysis to Taiyo Nippon Sanso Corporation (Tokyo, Japan). The levels of ¹⁸O₂ in treated cells were measured using stable isotope-ratio mass spectrometry. The results are shown as delta ‰ compared with the standard mean ocean water (¹⁸O₂ SMOW ‰).

2.4 | Immunofluorescence

Cells were cultured in glass-bottomed dishes using RPMI 1640 with or without 50 μmol/L H₂O₂ for 1 and 2 h. Subsequently, the cells were fixed with 4% formaldehyde in PBS for 30 min, and rinsed three times with PBS. Plasma membranes were permeabilized by incubation in 95% ethanol with 5% acetic acid for 10 min. After washing five times with PBS, cells were incubated for 30 min in blocking solution (5% skimmed milk in PBS-T; PBS with 0.05% Tween 20). The primary antibodies (incubated at 4°C overnight) were mouse anti-HNE (1:200 dilution; Japan institute for the control of aging, Shizuoka, Japan),

rabbit anti-PINK1, anti-aquaporin11, anti-ALOX5, anti-ALOX12, and anti-ALOX15 antibodies (Novus Biologicals, Centennial, CO, USA: BC100-494; ABGENT San Diego, CA, USA: AP58056; Abcam, Cambridge, UK: ab169755, ab211506, and ab80221; 1:1000 dilution), mouse anti-COX1 (Abcam: ab695; 1:500 dilution), and rabbit anti-COX2 (Abcam: ab15191; 1:100 dilution). The secondary antibodies (1:200 dilution, incubated at room temperature for 1 h) were the Alexa Fluor 488 goat anti-mouse IgG and Alexa Fluor 568 goat anti-rabbit IgG (Thermo Fisher Scientific, Waltham, MA, USA: A11001, and A11011). For staining the nuclei, cells were incubated with DAPI (0.5 µg/mL) at room temperature for 10 min. A BZ-8000 fluorescence microscope was used to obtain fluorescence images, and the ImageJ software was used to measure fluorescence intensity.

2.5 | Liposome assay

Liposomes containing luminol and horseradish peroxidase (HRP) were prepared as follows: DOPC (Avanti Polar Lipids Inc., Alabaster, AL, USA) and POVPC (Avanti Polar Lipids Inc.) were dissolved in chloroform (1 mg/mL) and mixed together. The dissolved lipids were dried to remove the chloroform. Subsequently, the mixture was added to 50 mmol/L Tris-HCl (pH 8.6) buffer containing 10 mmol/L luminol (Nacalai Tesque Inc.: 20751-34) and 100 µmol/L HRP (Wako Pure Chemical Industries Ltd.: 169-10791) and was then sonicated. The diameter of the prepared liposomes was calculated via the Dynamic Light Scattering method using ELS-Z2M (Otsuka Electronics Co. Ltd., Osaka, Japan). Subsequently, 8.8 mmol/L H₂O₂ were administered to the liposomes, and luminescence was observed using a luminometer (JASCO, Tokyo, Japan: FP-6300). Passage of H₂O₂ through the liposome membrane resulted in luminol reaction, producing blue luminescence.

2.6 | Administration of oxidized lipid

POVPC (12.5-50 µmol/L) was administered to the cultured medium using the ethanol injection method.^{27,28} This lipid has been shown to localize to the plasma membrane.^{27,28} After 10 min (SAS) or 30 min (HeLa) of treatment, POVPC was removed, and the cells were treated with 25 µmol/L H₂O₂ for 48 h. After administration of POVPC and H₂O₂, cell survival was analyzed using the CCK-8 assay kit (Dojindo Molecular Technologies, Inc., Kumamoto, Japan), as previously described.¹⁷

2.7 | Quantitative PCR

Total RNA was extracted using ISOGEN (Nippon Gene, Toyama, Japan), and reverse transcription was performed as previously described.¹⁷ cDNA equivalent to 1 ng of total RNA was used for the Quantitative PCR (qPCR). The reactions were performed with Step One Plus (Applied Biosystems; Foster City, CA, USA) using THUNDERBIRD[®] qPCR Mix (TOYOBO, Osaka, Japan). β -actin was used as the loading control. For the amplification of genes, one cycle of denaturation (95°C for 10 min) was performed, followed by 40

cycles of amplification (95°C for 10 s and 60°C for 60 s). Each experiment was performed in triplicate. Table 1 lists the primer sequences used in this experiment.

2.8 | Western blotting

Each cell lysate (30 µg per lane) was subjected to SDS-PAGE under reduced conditions using a 10% or 15% polyacrylamide gel. The proteins were subsequently blotted on a PVDF membrane. After blocking with blocking buffer (3% skimmed milk in TBS-T; TBS with 0.05% Tween 20, for ALOX12 antibody and 5% skimmed milk in PBS-T for the other primary antibodies), the blotted membranes were incubated with primary antibodies (rabbit anti-ALOX5, anti-ALOX12, anti-ALOX15, mouse anti-COX1, rabbit anti-COX2; Abcam: ab169755, ab211506, ab80221, ab695, and ab15191, rabbit anti-Akt, pAkt^{T308}, pAkt^{S473}, FOXO1, pGSK3 β ^{S9}; Cell Signaling Technology, Danvers, MA, USA: #4691, #13038, #4060, #2880, #5558, mouse anti-BCL2, Bax; Santa Cruz Biotechnology, San Diego, CA, USA: SC-7382, SC-7480) in blocking buffer at 4°C overnight. After five washes with TBS-T (ALOX12 antibody) or PBS-T (other antibodies), the membranes were incubated with peroxidase-conjugated anti-rabbit IgG antibody or anti-mouse IgG antibodies (GE Healthcare UK Ltd., Amersham Place, England) at room temperature for 2 h. Immunoreactive proteins were visualized with ECL prime (GE Healthcare) using ChemiDoc XRS Plus (BIORAD Laboratories, Inc., Hercules, CA, USA). An anti- β -actin antibody (Novus Biologicals LLC, Centennial, CO, USA; NB100-56874) was used as loading control. The dilution factor for all antibodies was 1:1000. Table 2 represents the mean and standard error of the mean (SEM) of three independent ρ^0 /parent intensity ratios after normalization against β -actin.

2.9 | ALOX inhibitor assay

Cells were treated with 10 µmol/L caffeic acid (Nacalai Tesque Inc.), the ALOX5 inhibitor, or 10 µmol/L NDGA (Sigma-Aldrich), the

TABLE 1 Primer sequences

Primer name	Primer sequence
ALOX5 F	5'-CTGGGCATGTACCCAGAAGAGCATTTTAT-3'
ALOX5 R	5'-ACAAGTAGTAATATGGCAGCTGCTTCTTCT-3'
ALOX12 F	5'-TCAAATGGCCATCTCATGGCATCTGAGT-3'
ALOX12 R	5'-ATCTGTTCGGAATTGGTTTAGCACAGCTTT-3'
ALOX15 F	5'-ATCTATCGGTATGTGGAAGGAATCGTGAGT-3'
ALOX15 R	5'-TAAAGAGACAGGAAACCCTCGGTCCT-3'
COX1 F	5'-AATCCCATCTGTTCTCCGGAGTACTG-3'
COX1 R	5'-GAAACGTAGGGACAGGTCTTGGTGTT-3'
COX2 F	5'-TGGAGCACCATTCTCCTTGAAAGGACTTAT-3'
COX2 R	5'-GACTGTTTTAATGAGCTCTGGATCTGGAAC-3'
β -Actin F	5'-AGAGCTACGAGCTGCCTGAC-3'
β -Actin R	5'-AGCACTGTGTTGGCGTACAG-3'

TABLE 2 Relative levels of protein expression in HeLa and SAS ρ^0 /parent cells (n = 3)

	ρ^0 /parent	SEM
ALOX5		
HeLa	0.61	.16
SAS	0.61	.01
ALOX12		
HeLa	1.51	.14
SAS	1.24	.05
ALOX15		
HeLa	1.42	.04
SAS	1.24	.05
COX1		
HeLa	1.14	.01
SAS	1.08	.05
COX2		
HeLa	0.53	.14
SAS	0.36	.05
Akt		
HeLa	0.87	.07
SAS	1.00	.01
pAkt ^{T308}		
HeLa	0.64	.13
SAS	0.49	.20
pAkt ^{S473}		
HeLa	0.52	.17
SAS	0.63	.14
FOXO1		
HeLa	1.44	.17
SAS	1.28	.07
GSK3 β ^{S9}		
HeLa	0.71	.11
SAS	0.72	.16
BCL2		
HeLa	0.78	.00
SAS	0.67	.11
Bax		
HeLa	1.88	.04
SAS	1.31	.01

nonspecific ALOXs inhibitor, at 37°C for 10 min. After removal of the inhibitor-containing medium, the cells were treated with 50 μ mol/L H₂O₂ for 1 h. HYDROP™ and HNE antibody were used as described above to detect internal H₂O₂ or HNE.

2.10 | Detection of OH using HPF

Internal levels of \cdot OH were detected using HPF (Goryo Chemical Inc.) according to the protocol provided by the manufacturer with

slight modification. HPF (10 μ mol/L) with MIC buffer (130 mmol/L sodium chloride, 5.3 mmol/L potassium chloride, 0.8 mmol/L magnesium sulfate, 1 mmol/L disodium phosphate, 2 mmol/L glucose, 20 mmol/L HEPES, 1 mmol/L sodium pyruvate, 2.5 mmol/L sodium bicarbonate, 1 mmol/L ascorbic acid, 1.5 mmol/L calcium chloride, and 1.5 mg/mL bovine serum albumin (BSA)) was added to the cells in glass-bottomed dishes. After incubation at 37°C for 15 min, the HPF with MIC buffer was replaced with new MIC buffer. Images were obtained using a BZ-8000 fluorescence microscope. Nuclei were counterstained with DAPI as described above.

2.11 | Statistical analysis

One-way analysis of variance with Scheffe's F test was performed for the water-soluble tetrazolium assay and ALOX inhibitor experiment. All other statistical analyses were performed using Student's t test. A $P < .05$ denoted statistical significance. The results were expressed as means \pm SEM.

3 | RESULTS

3.1 | Relative levels of internal H₂O₂ and intake of H₂O₂

After treatment for 1 h, the internal levels of H₂O₂ were increased only in ρ^0 vs parental cells (Figure 1A). The results obtained from the treatment with ¹⁸O₂-labeled H₂O₂ showed that the intake of H₂O₂ in ρ^0 cells was significantly higher than that observed in parental cells after treatment with H₂O₂ for 1 h (Figure 1B).

3.2 | Timing of increase in lipid peroxidation and internal levels of H₂O₂

Significantly higher intensity was observed in ρ^0 cells (Figure 2A, B). Co-staining with PINK1 (localized in mitochondria) and aquaporin 11 (localized in the plasma membrane) revealed that HNE was mainly localized in the plasma membrane (Figure 2C, D). Moreover, temporal change of lipid peroxidation was observed to investigate the timing of this process after treatment with H₂O₂ (Figure 2E). Lipid peroxidation was increased 1 h after treatment (Figure 2E, F), whereas the internal levels of H₂O₂ were increased in parental cells 2 h after treatment (Figure 2F).

3.3 | H₂O₂ permeability using liposome and administration of oxidized lipid

We prepared liposomes encapsulating luminol and HRP to quantify the permeation of H₂O₂. Representative phospholipids of the plasma membrane (ie, DOPC and oxidized lipid POVPC) were used in this model. Internal levels of H₂O₂ can be detected as luminescence of luminol catalyzed by HRP (Figure 3A). The intensity of luminescence was increased following the administration of H₂O₂. Differential DOPC/POVPC ratio liposomes were prepared to investigate

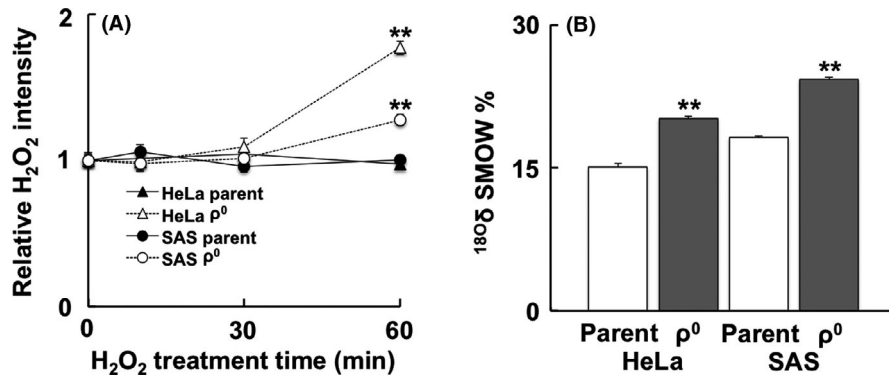


FIGURE 1 Internal levels of H₂O₂ and intracellular intake of H₂O₂ in ρ⁰ cells. A, Temporal change of H₂O₂ after treatment with H₂O₂ in ρ⁰ and parental cells using HYDROP™. In ρ⁰ cells, the relative H₂O₂ intensity was increased after treatment with H₂O₂ for 1 h. B, The intracellular intake of H₂O₂ was detected using a stable isotope. Cells were subjected to 50 μmol/L of H₂O₂ ¹⁸O₂ solution, and the content of ¹⁸O₂ was measured using stable isotope-ratio mass spectrometry. In ρ⁰ cells, the intake of H₂O₂ was significantly higher than that observed in parental cells after treatment. The results are expressed as the mean ± SEM. ***P* < .01 using Student's *t* test

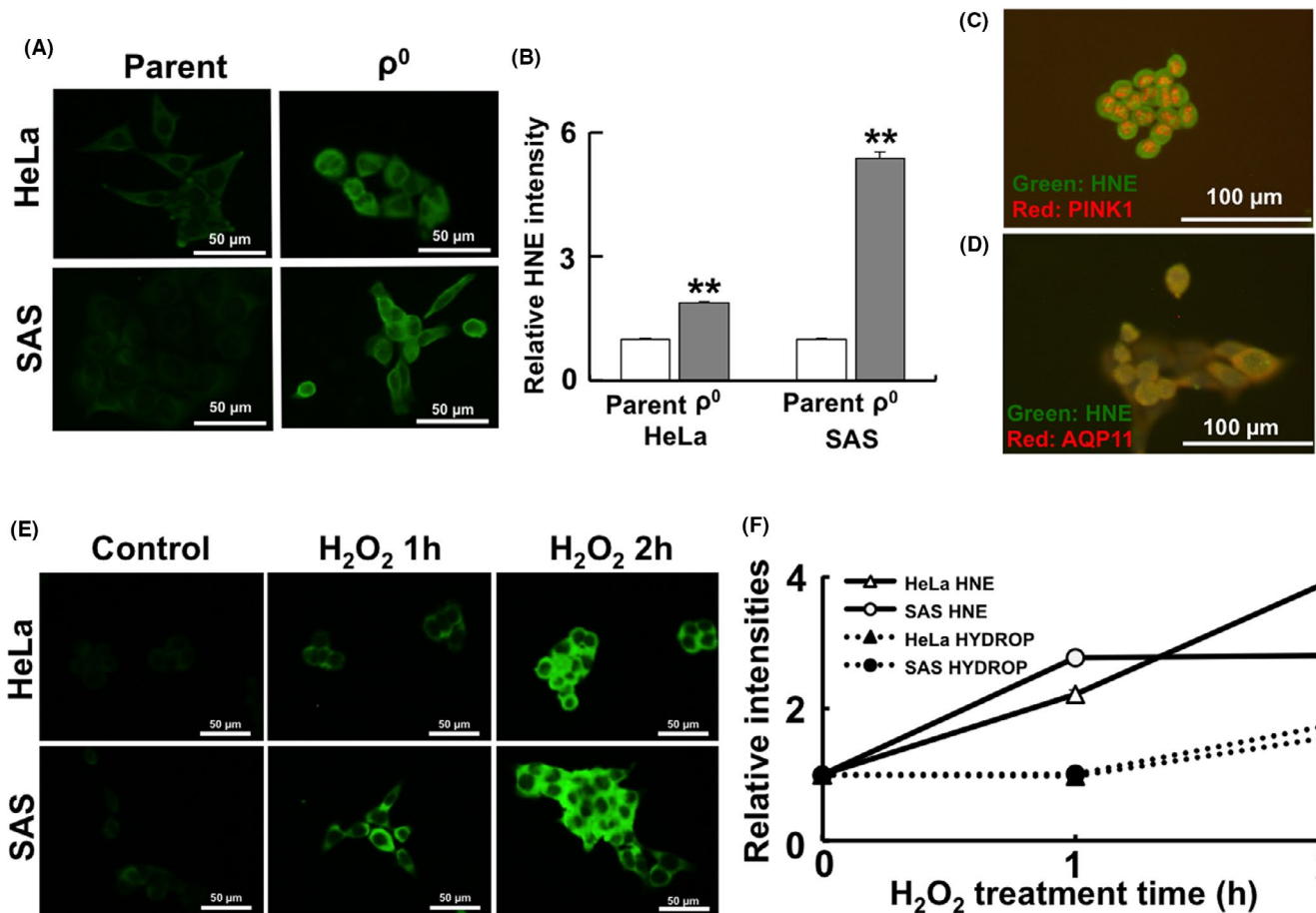


FIGURE 2 Timing of increase in lipid peroxidation and internal H₂O₂ levels. A, Immunofluorescence images of 4-hydroxynonenal (HNE). B, Relative HNE intensity. (C, D) HNE staining with PINK1 (localized in the mitochondria, C) and AQP11 (localized in the plasma membrane, D). HNE was mainly co-localized with AQP11 that is present in the plasma membrane. E, Immunofluorescence images of HNE in HeLa and SAS parental cells after treatment with H₂O₂. F, Timing of lipid peroxidation and internal H₂O₂ levels. The results are expressed as the mean ± SEM. ***P* < .01 using Student's *t* test

changes in H₂O₂ permeability. Maximum H₂O₂ transport appeared in the presence of several (2-4) mol% of POVPC (Figure 3B). The POVPC administration experiment was conducted to confirm

whether administration of this oxidized lipid led to cell death. The results showed that the administration of 12.5 μmol/L POVPC significantly increased the sensitivity of HeLa and SAS parental cells to

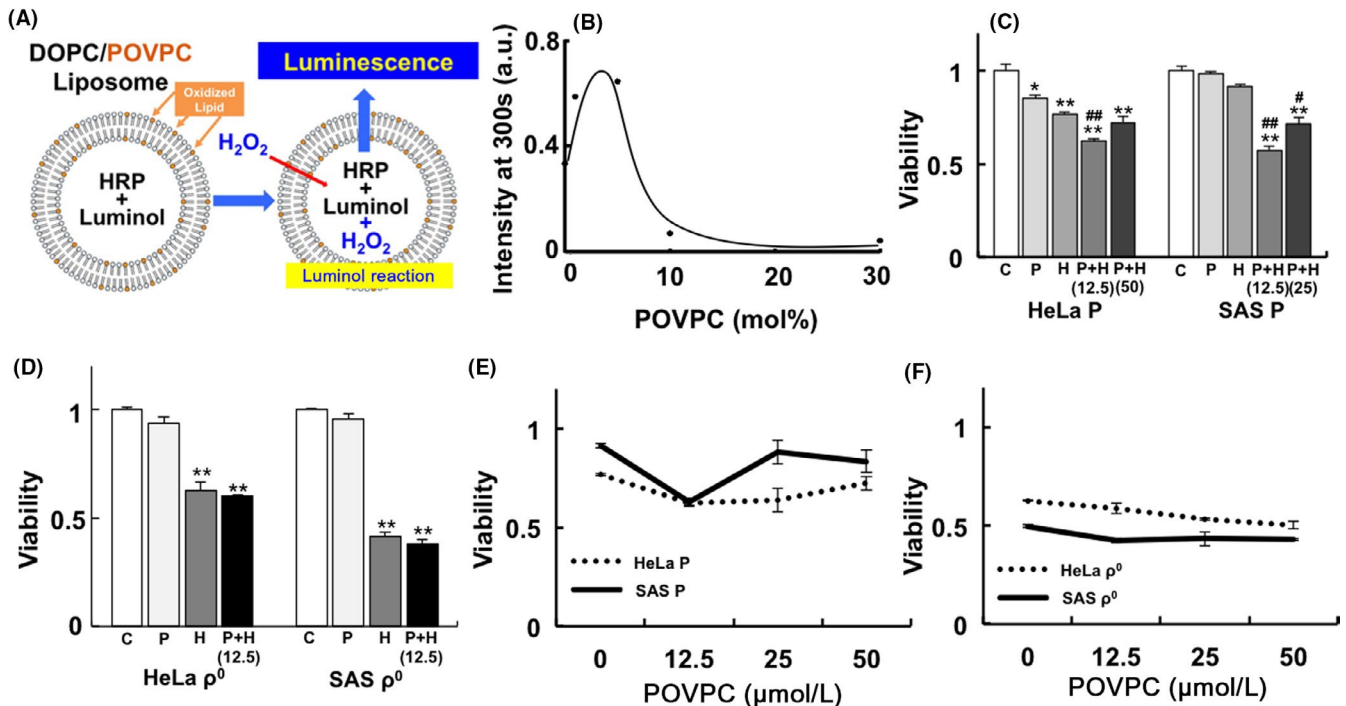


FIGURE 3 H_2O_2 permeability using liposome and administration of oxidized lipid. A, Structure of the liposome. The representative phospholipids of the plasma membrane (ie, 1,2-dioleoyl-sn-glycero-3-phosphocholine (DOPC) and oxidized lipid 1-palmitoyl-2-(5'-oxo-valeroyl)-sn-glycero-3-phosphocholine (POVPC)) were used. B, Effect of the oxidized lipid ratio to the H_2O_2 permeability of the liposome. Up to several (2-4) mol%, the administration of oxidized lipid increased H_2O_2 permeability. C, D, Administration of oxidized lipid in HeLa and SAS parental (C) or ρ^0 (D) cells before H_2O_2 treatment. The numbers in parentheses represent the concentration of POVPC ($\mu\text{mol/L}$). E, F, Effect of the concentration of POVPC on the viability of HeLa and SAS parental (E) or ρ^0 (F) cells before H_2O_2 treatment (25 $\mu\text{mol/L}$). The results are expressed as the mean \pm SEM. * $P < .05$, ** $P < .01$ using Scheffe's F test (vs control), # $P < .05$, ## $P < .01$ using Scheffe's F test (vs treatment with H_2O_2). C: control, P: treatment with POVPC (12.5 $\mu\text{mol/L}$), H: treatment with H_2O_2 (25 $\mu\text{mol/L}$ for 48 h), P+H: treatment with H_2O_2 after treatment with POVPC

H_2O_2 . However, a higher concentration of POVPC did not induce a similar increase in sensitivity to H_2O_2 (Figure 3C). Furthermore, administration of different concentrations of POVPC revealed that the relationship between cell viability and POVPC concentration did not show a linear concentration-dependent pattern. However, it showed a reverse bell shape, with the lowest viability in HeLa and SAS parental cells observed after the administration of 12.5 $\mu\text{mol/L}$ POVPC (Figure 3D). In contrast, administration of 12.5 $\mu\text{mol/L}$ POVPC did not increase sensitivity to H_2O_2 . The relationship between cell viability and the concentration of POVPC showed a linear concentration-dependent pattern in HeLa and SAS ρ^0 cells that contained more oxidized lipid before treatment (Figure 3E, F).

3.4 | Gene expression and protein expression of ALOX

Gene expression of *ALOX5*, *ALOX12*, and *ALOX15* – involved in lipid peroxidation of the plasma membrane – was upregulated in ρ^0 cells (Figure 4A: *ALOX5*, 4B: *ALOX12*, and 4C: *ALOX15*). In addition, protein expression of *ALOX12* and *ALOX15*, unlike that of *ALOX5*, was upregulated in both HeLa and SAS ρ^0 cells (Figure 4D and Table 2). Investigation of spatial distribution showed that the *ALOX12* and *ALOX15* proteins were distributed in the nucleus and cytoplasm. Conversely, the *ALOX5*

protein was distributed only in the nucleus (Figure S1). A semiquantitative analysis of immunofluorescence revealed that the relative expression of the *ALOX12* and *ALOX15* proteins was upregulated in ρ^0 cells (Figure 5A, C: *ALOX12*, Figure 5B, D: *ALOX15*).

3.5 | Inhibition of ALOX

Treatment with 10 $\mu\text{mol/L}$ caffeic acid (*ALOX-5* inhibitor) or 10 $\mu\text{mol/L}$ NDGA (universal *ALOX* inhibitor) was performed before treatment with H_2O_2 to investigate the effect of *ALOX* on the levels of internal H_2O_2 or HNE. The results showed that, unlike caffeic acid, NDGA significantly inhibited the levels of internal H_2O_2 and lipid peroxidation (Figure 6).

3.6 | Gene and protein expressions of COX

Expression of the *COX1* gene was downregulated in SAS ρ^0 cells (Figure 7A). Conversely, expression of the *COX2* gene was significantly upregulated in HeLa and SAS ρ^0 cells (Figure 7B). Protein expression of *COX1* did not change significantly between parental and ρ^0 cells, whereas that of *COX2* was downregulated in ρ^0 cells (Figure 7C and Table 2). Immunofluorescence of *COX* revealed that *COX1* was mainly localized in the nucleus, whereas *COX2* was mainly localized in the cytoplasm (Figure 7D).

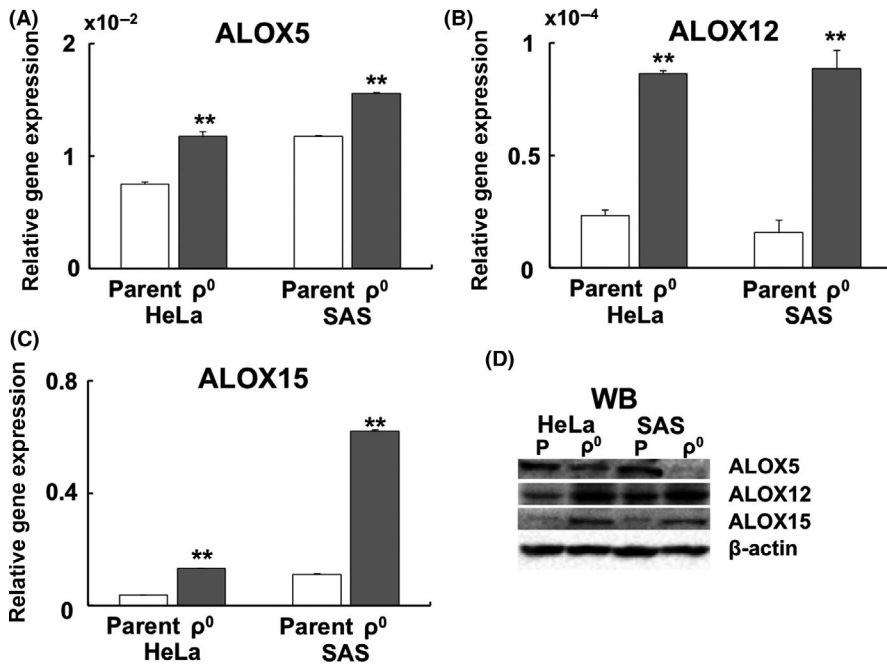


FIGURE 4 Expression of the ALOX gene and protein in ρ^0 cells. A, Expression of the ALOX5 gene. B, Expression of the ALOX12 gene. C, Expression of the ALOX15 gene. The results are expressed as the mean \pm SEM. ** $P < .01$ using Student's *t* test. D, Western blotting of ALOX5, ALOX12, and ALOX15. Unlike ALOX5, the expression of ALOX12 and ALOX15 was upregulated in HeLa and SAS ρ^0 cells

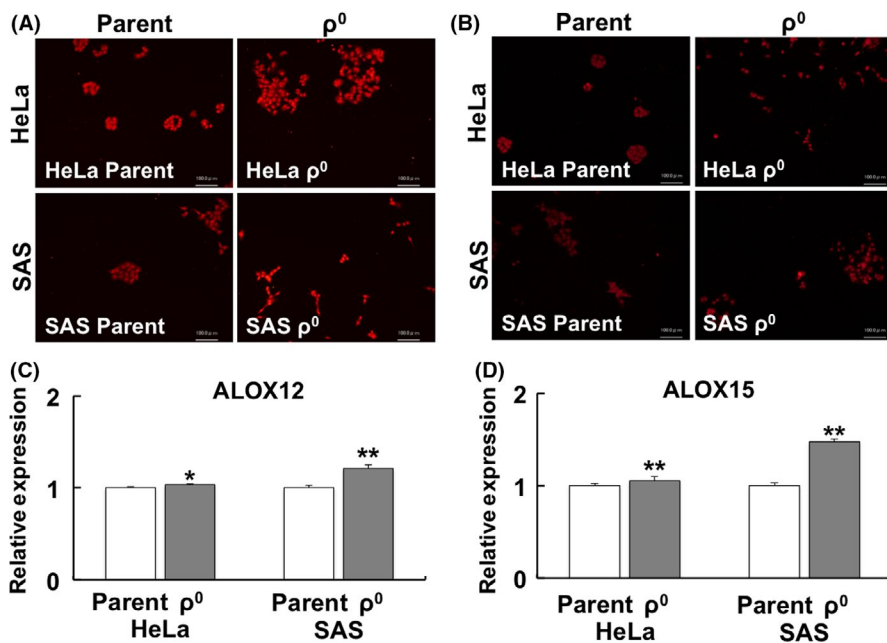


FIGURE 5 Immunofluorescence of ALOX12 and ALOX15. A, B, Spatial distribution of ALOX12 (A) and ALOX15 (B). C, D, Relative expression of ALOX12 (C) and ALOX15 (D). The results are expressed as the mean \pm SEM. * $P < .05$, ** $P < .01$ using Student's *t* test

3.7 | Phosphorylation of Akt and protein expressions involved in apoptosis

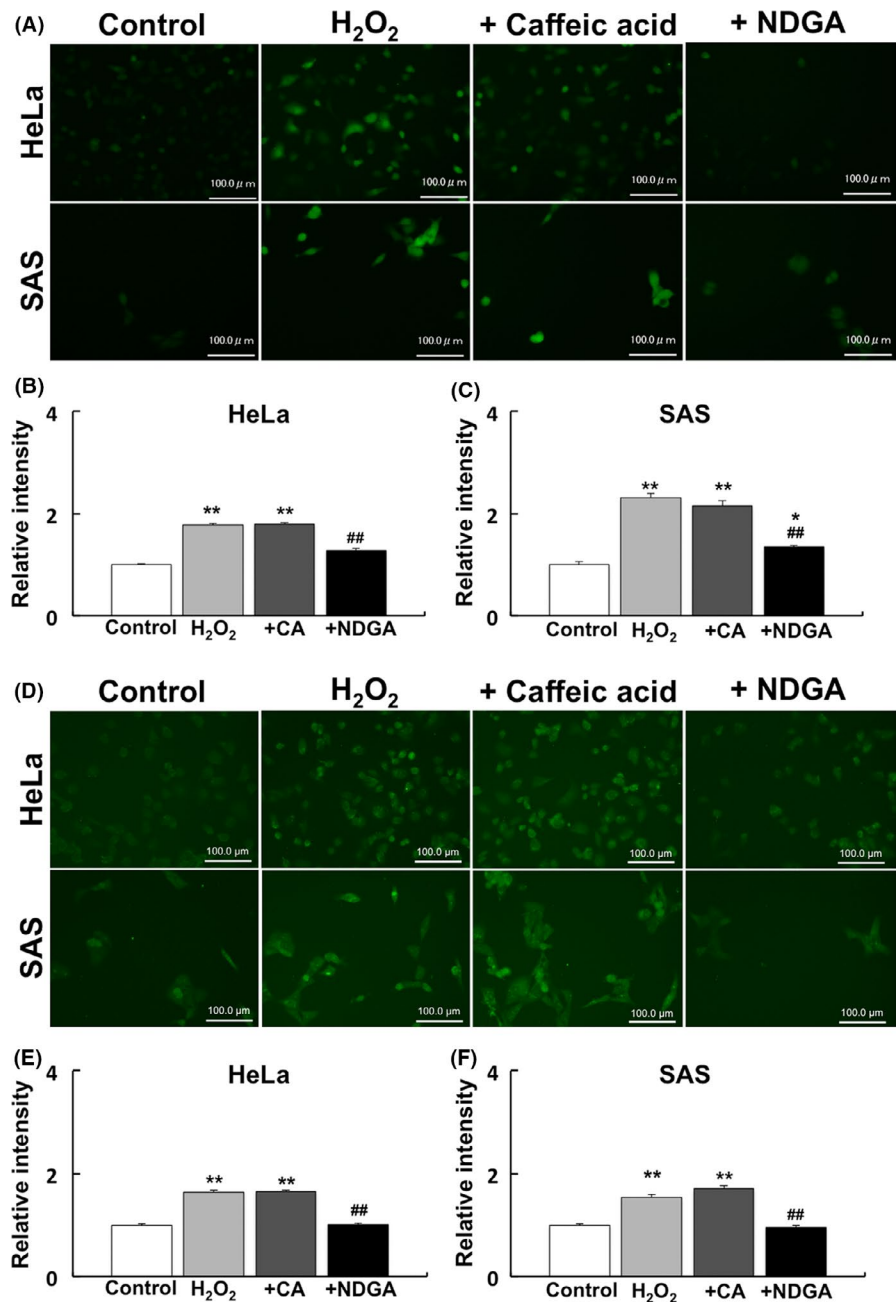
Phosphorylation of Akt, which inhibits apoptosis and regulates cell proliferation, was investigated using western blotting. This analysis revealed a marked decrease in Akt phosphorylation in ρ^0 cells (Figure 8 and Table 2). Expression of Akt downstream proteins was also investigated. Expression of FOXO1, which is downregulated by Akt phosphorylation and inhibited apoptosis, was increased. Moreover, pGSK3 β ^{S9}, which is the inactivated form of GSK3 β , was decreased in ρ^0 cells. Expression of the anti-apoptotic protein BCL2 was decreased, whereas expression of the

apoptosis-inducing protein Bax was increased in ρ^0 cells (Figure 8 and Table 2).

4 | DISCUSSION

The present results indicated that the susceptibility of ρ^0 cells to H₂O₂ may be attributed to an increase in the levels of intracellular ROS due to peroxidation of the plasma membrane. ρ^0 cells from osteosarcomas have previously shown sensitivity to X-ray irradiation and produced more ROS from mitochondria than their parental cells.^{14,19} Similarly, lung carcinoma ρ^0 cells have shown sensitivity

FIGURE 6 Effect of ALOX inhibitor on internal H_2O_2 and lipid peroxidation. Treatment with 10 $\mu\text{mol/L}$ caffeic acid (ALOX-5 inhibitor) or 10 $\mu\text{mol/L}$ nordihydroguaiaretic acid (NDGA) (universal ALOX inhibitor) was performed to investigate their effect on internal H_2O_2 and lipid peroxidation. A, Immunofluorescence images of internal H_2O_2 . B, C, Relative intensity of internal H_2O_2 in HeLa (B) and SAS cells (C). D, Immunofluorescence images of 4-hydroxynonenal (HNE). E, F, Relative intensity of internal H_2O_2 in HeLa (E) and SAS (F) cells. Control: no treatment. H_2O_2 : treatment with 50 $\mu\text{mol/L}$ H_2O_2 . +CA: treatment with 10 $\mu\text{mol/L}$ caffeic acid before treatment with 50 $\mu\text{mol/L}$ H_2O_2 . +NDGA: treatment with 10 $\mu\text{mol/L}$ NDGA before treatment with 50 $\mu\text{mol/L}$ H_2O_2 . The results are expressed as the mean \pm SEM. * $P < .05$, ** $P < .01$ using Scheffe's F test (vs control), ## $P < .01$ using Scheffe's F test (vs treatment with H_2O_2)



to X-ray irradiation by decreasing the expression of CuZn-SOD.¹⁹ Conversely, ρ^0 cells may be resistant to oxidative stress; and ρ^0 cells from GM701 and BEAS-2B have shown resistance to irradiation.^{19,20} Additionally, GM701 ρ^0 and BEAS-2B ρ^0 cells have shown resistance through inhibition of apoptosis and reduction of DNA damage, respectively. However, in these cell lines, intracellular levels of ROS were not determined. Therefore, it remained unknown whether ρ^0 cells exhibited resistance to ROS, such as H_2O_2 . Collectively, the increased production of internal ROS via oxidative stress may lead to increased cell death in ρ^0 cells.

In our study, liposome membrane experiments showed that the content of oxidized lipid in liposomes increased H_2O_2 permeability by at least several (2-4) mol% (Figure 3A, B). Administration of oxidized lipid to HeLa and SAS parent cells produced a decrease

in cell viability following treatment with H_2O_2 (Figure 3C, D). The reduced cell viability induced by 12.5 $\mu\text{mol/L}$ POVPC may reflect the results of the liposome experiments. As shown in Figure 3B, the highest uptake of H_2O_2 was caused at a POVPC concentration of several (2-4) mol%, and administration of 12.5 $\mu\text{mol/L}$ POVPC (Figure 3D) induced marked cell damage. In contrast, the administration of oxidized lipid did not affect cell viability following treatment with H_2O_2 in ρ^0 cells, in which lipid peroxidation was enhanced (Figure 3E, F). From these results, the concentration of the oxidized lipids was thought to influence H_2O_2 permeability and viability. However, administration of oxidized lipids to parental cells whose plasma membrane was not highly oxidized, is effective in inducing cell death after treatment with H_2O_2 . Recently, it was reported that the density of phospholipids in the plasma membrane

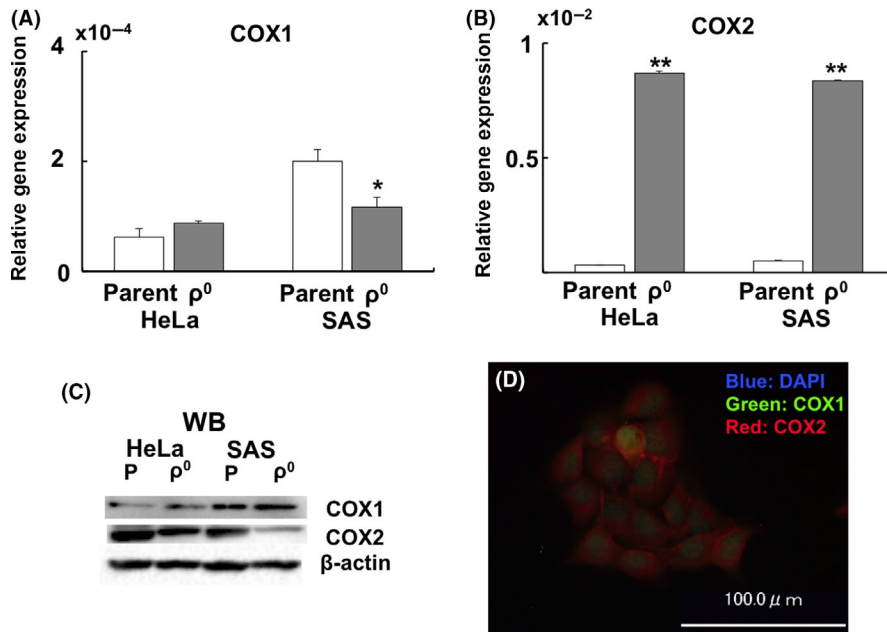


FIGURE 7 Gene and protein expression of COX. A, Relative gene expression of COX1. B, Relative gene expression of COX2. C, Western blotting of COX1 and COX2. D, Spatial distribution of COX1 (green) and COX2 (red) in SAS parent cells. The results are expressed as the mean \pm SEM. * $P < .05$, ** $P < .01$ using Student's *t* test

is involved in the efficiency of membrane permeability (ie, uptake of ions or low-molecular-weight substances, such as H_2O_2).²⁹ The results of our liposome experiment are in accordance with those findings reported by a recent study,²⁹ suggesting that different densities of POVPC influence H_2O_2 membrane permeability. Uptake of H_2O_2 may be largely related to changes in the plasma membrane itself, rather than the presence of functional proteins on the membrane (ie, aquaporins) that are involved in the permeation of H_2O_2 into the cell.³⁰⁻³³

In HeLa and SAS ρ^0 cells, lipid peroxidation in the plasma membrane was higher than that observed in parental cells. The following three factors may be involved in lipid peroxidation and cell death: (a) downregulation of the antioxidant enzymes; (b) upregulation of the endogenous levels of ROS; and (c) upregulation of intracellular oxidase. It has been reported that catalase activity and expression of the *Mn-SOD* gene were upregulated in ρ^0 cells. In addition, expression of the *GPx1* gene was downregulated in SAS ρ^0 cells, whereas it was upregulated in HeLa ρ^0 cells.¹⁷ In osteosarcoma, rhabdomyosarcoma, and lung ρ^0 cells, glutathione peroxidase activity and the expression levels of the *Mn-SOD* and *CuZn-SOD* genes were upregulated. However, expression of the *CuZn-SOD* protein in osteosarcoma ρ^0 cells was downregulated.³⁴ These results suggested that antioxidant enzymes are not the main factors involved in lipid peroxidation in ρ^0 cells. It has been reported that the levels of superoxide from the mitochondria are decreased in ρ^0 cells.³⁵

Moreover, it has been reported that the administration of HNE leads to increased levels of internal ROS using 2',7'-dichlorodihydrofluorescein diacetate in parental cells. However, the levels of internal ROS in ρ^0 cells did not increase significantly.³⁶ Our data showed that the levels of HNE and $\cdot OH$ were increased in ρ^0 cells (Figures 2 and S2). Currently, the involvement of mitochondria-derived ROS in lipid peroxidation of the plasma membrane in ρ^0 cells remains unknown.

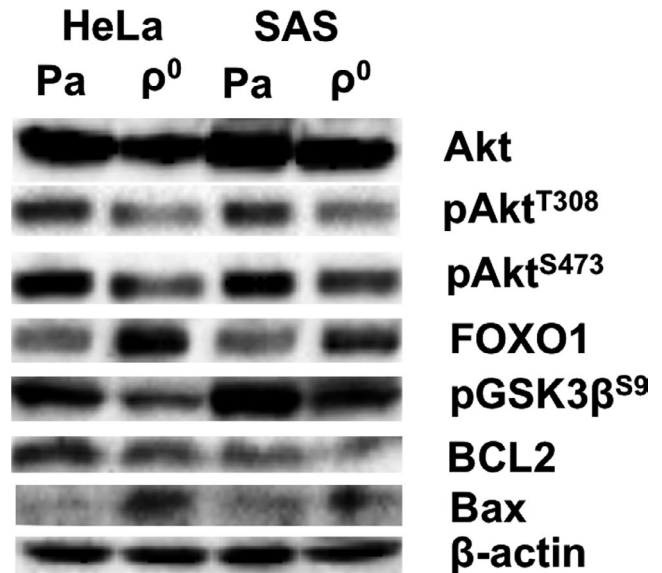


FIGURE 8 Downregulation of Akt phosphorylation and promotion of apoptosis signaling in ρ^0 cells. Western blots of Akt, pAkt^{T308}, pAkt^{S473}, FOXO1, pGSK3 β ^{S9}, BCL2, Bax, and β -actin are shown. Downregulation of Akt phosphorylation was observed in both HeLa and SAS ρ^0 cells. The expression of apoptosis-promoting proteins (FOXO1 and Bax) was upregulated, whereas that of apoptosis-inhibiting proteins (pGSK3 β ^{S9} and BCL2) was downregulated

It has been reported that an increase in $\cdot OH$ from the mitochondria was detected in osteosarcoma ρ^0 cells.¹⁴ Additionally, it has been reported that $\cdot OH$ in cells was involved in the initiation of lipid peroxidation.³⁷ Moreover, H_2O_2 reportedly produced $\cdot OH$ in the presence of ferrous ion, leading to lipid peroxidation and cell death.³⁸ These results indicated a positive correlation between the levels of $\cdot OH$ and lipid peroxidation of the plasma membrane in ρ^0 cells.

The expression of ALOX12 and ALOX15 (mRNA and protein levels) and COX2 was upregulated in ρ^0 cells (Figure 4-7). ALOX15 produces 13-hydroxyoctadecadienoic acid, which is a precursor of HNE from linoleic acid.³⁹ Inhibition of ALOX 12 and 15, unlike ALOX5, resulted in the downregulation of HNE and H_2O_2 permeability in ρ^0 cells (Figure 6). Moreover, overexpression of ALOX15 enhanced erastin and RAS-selective lethal compound 3-induced ferroptosis, an iron-dependent cell death via activation of the HNE.⁴⁰ Furthermore, ALOX15 reportedly plays a central role in the initiation and execution of ferroptosis.⁴¹ These results suggested that the expression of internal oxidative enzymes is more important than that of antioxidative enzymes for lipid oxidation in ρ^0 cells. Additionally, ALOX15 plays an important role in the peroxidation of the plasma membrane in ρ^0 cells. To date, there is no evidence showing that COX2 directly peroxidizes lipids and produces HNE. However, it has been reported that HNE induces the expression of the COX2 gene, and that this expression is stabilized by the p38 mitogen-activated protein kinase.⁴² In addition, COX2 has been reported to be involved in PI3K/Akt signaling.⁴³ Recently, it was reported that administration of HNE decreased Akt phosphorylation and induced apoptosis in an osteosarcoma cell line.⁴⁴ These findings indicated a strong relationship between lipid peroxidation and intracellular signal pathways (eg, Akt signaling). It has been shown that phosphorylation of Akt was downregulated in HeLa ρ^0 cells.⁴⁵ Our results showed that Akt phosphorylation was downregulated in both types of ρ^0 cells (Figure 8). Moreover, an apoptosis-promoting signal was activated in ρ^0 cells (Figure 8 and Table 2). These results indicated that the downregulation of Akt phosphorylation promoted cell death (ie, apoptosis and/or ferroptosis) in ρ^0 cells via upregulation of COX2.

In conclusion, the sensitivity of ρ^0 cells to treatment with H_2O_2 may be due to peroxidation of the plasma membrane, leading to increases in H_2O_2 permeability and cell death. Moreover, alterations in the state of the membrane may change the susceptibility of cells to drugs. These findings offer promise for the development of novel anticancer drugs, altering the oxidation state of the plasma membrane. Such drugs may be helpful in overcoming resistance to RT and drug therapy in cells.

ACKNOWLEDGMENTS

This work was supported by a Grant from the Kodama Memorial Fund for Medical Research to KT and JSPS KAKENHI (Grant-in Aid for Scientific Research C: no. 16K11513 to KT; 16K00538 to YK). The authors would like to thank Enago (www.enago.jp) for English language review.

CONFLICT OF INTEREST

The authors declare that there is no conflict of interest.

ORCID

Kazuo Tomita  <https://orcid.org/0000-0003-1266-7948>

REFERENCES

- Zou Z, Chang H, Li H, et al. Induction of reactive oxygen species: an emerging approach for cancer therapy. *Apoptosis*. 2017;22:1321-1335.
- Dong J, Liu B, Zhu R. Targeting ROS for cancer therapy. *Chemo Open Access*. 2016;5:2.
- Tarlovsky VF. Role of antioxidants in cancer therapy. *Nutrition*. 2013;29:15-21.
- Tada-Oikawa S, Oikawa S, Kawanishi M, et al. Generation of hydrogen peroxide precedes loss of mitochondrial membrane potential during DNA alkylation-induced apoptosis. *FEBS Lett*. 1999;442:65-69.
- Varbiro G, Veres B, Gallyas F Jr, et al. Direct effect of Taxol on free radical formation and mitochondrial permeability transition. *Free Radic Biol Med*. 2001;31:548-558.
- Murata M, Suzuki T, Midorikawa K, et al. Oxidative DNA damage induced by a hydroperoxide derivative of cyclophosphamide. *Free Radic Biol Med*. 2004;37:793-802.
- Magda D, Miller RA. Motexafin gadolinium: a novel redox active drug for cancer therapy. *Semin Cancer Biol*. 2006;16:466-476.
- Alexandre J, Nicco C, Chéreau C, et al. Improvement of the therapeutic index of anticancer drugs by the superoxide dismutase mimics mangafodipir. *J Natl Cancer Inst*. 2006;98:236-244.
- Trachootham D, Alexandre J, Huang P. Targeting cancer cells by ROS-mediated mechanisms: a radical therapeutic approach? *Nat Rev Drug Discov*. 2009;8:579-591.
- Fang Y, Moore BJ, Bai Q, et al. Hydrogen peroxide enhances radiation-induced apoptosis and inhibition of melanoma cell proliferation. *Anticancer Res*. 2013;33:1799-1807.
- Kariya S, Sawada K, Kobayashi T, et al. Combination treatment of hydrogen peroxide and X-rays induces apoptosis in human prostate cancer PC-3 cells. *Int J Radiat Oncol Biol Phys*. 2009;75:449-454.
- Forman HJ, Torres M. Reactive oxygen species and cell signaling: respiratory burst in macrophage signaling. *Am J Respir Crit Care Med*. 2002;166:S4-S8.
- Ogura A, Oowada S, Kon Y, et al. Redox regulation in radiation-induced cytochrome c release from mitochondria of human lung carcinoma A549 cells. *Cancer Lett*. 2009;277:64e71.
- Indo HP, Davidson M, Yen H-C, et al. Evidence of ROS generation by mitochondria in cells with impaired electron transport chain and mitochondrial DNA damage. *Mitochondrion*. 2007;7:106-118.
- Chatterjee A, Mambo E, Sidransky D. Mitochondrial DNA mutations in human cancer. *Oncogene*. 2006;25:4663-4674.
- Lin MT, Beal MF. Mitochondrial dysfunction and oxidative stress in neurodegenerative diseases. *Nature*. 2006;443:787-795.
- Tomita K, Kuwahara Y, Takashi Y, et al. Sensitivity of mitochondrial DNA depleted ρ^0 cells to H_2O_2 depends on the plasma membrane status. *Biochem Biophys Res Commun*. 2017;490:330-335.
- Grant CM, MacIver FH, Dawes IW. Mitochondrial function is required for resistance to oxidative stress in the yeast *Saccharomyces cerevisiae*. *FEBS Lett*. 1997;410:219-222.
- van Gisbergen MW, Voets AM, Biemans R, et al. Distinct radiation responses after in vitro mtDNA depletion are potentially related to oxidative stress. *PLoS ONE*. 2017;12:e0182508.
- Tang JT, Yamazaki H, Inoue T, et al. Mitochondrial DNA influences radiation sensitivity and induction of apoptosis in human fibroblasts. *Anticancer Res*. 1999;19:4959-4964.
- Cloos CR, Daniels DH, Kalen A, et al. Mitochondrial DNA depletion induces radioresistance by suppressing G2 checkpoint activation in human pancreatic cancer cells. *Radiat Res*. 2009;171:581-587.
- Esterbauer H, Schaur RJ, Zollner H. Chemistry and biochemistry of 4-hydroxynonenal, malonaldehyde and related aldehydes. *Free Radic Biol Med*. 1991;11:81-128.

23. Uchida K. 4-Hydroxy-2-nonenal: a product and mediator of oxidative stress. *Progress Lipid Res.* 2003;42:318-343.
24. Ayala A, Muñoz MF, Argüelles S. Lipid peroxidation: production, metabolism, and signaling mechanisms of malondialdehyde and 4-hydroxy-2-nonenal. *Oxid Med Cell Longev.* 2014;2014:360438.
25. Bromfield EG, Mihalas BP, Dun MD, et al. Inhibition of arachidonate 15-lipoxygenase prevents 4-hydroxynonenal-induced protein damage in male germ cells. *Biol Reprod.* 2017;96:598-609.
26. Shi Q, Vaillancourt F, Côté V, et al. Alterations of metabolic activity in human osteoarthritic osteoblasts by lipid peroxidation end product 4-hydroxynonenal. *Arthritis Res Ther.* 2006;8:R159.
27. Tomita K, Kuwahara Y, Takashi Y, et al. Clinically relevant radioresistant cells exhibit resistance to H₂O₂ by decreasing internal H₂O₂ and lipid peroxidation. *Tumor Biol.* 2018;40:1010428318799250.
28. Batzri S, Korn ED. Single bilayer liposomes prepared without sonication. *Biochim Biophys Acta.* 1973;298:1015-1019.
29. Kobayashi D, Nakahara H, Shibata O, et al. Interplay of hydrophobic and electrostatic interactions between polyoxometalates and lipid molecules. *J Phys Chem C.* 2017;121:12895-12902.
30. Miller EW, Dickinson BC, Chang CJ. Aquaporin-3 mediates hydrogen peroxide uptake to regulate downstream intracellular signaling. *Proc Natl Acad Sci USA.* 2010;107:15681-15686.
31. Medraño-Fernandez I, Bestetti S, Bertolotti M, et al. Stress regulates aquaporin-8 permeability to impact cell growth and survival. *Antioxid Redox Signal.* 2016;24:1031-1044.
32. Al Ghouleh I, Frazziano G, Rodriguez AI, et al. Aquaporin 1, Nox1, and Ask1 mediate oxidant-induced smooth muscle cell hypertrophy. *Cardiovasc Res.* 2012;97:134-142.
33. Bienert GP, Møller AL, Kristiansen KA, et al. Specific aquaporins facilitate the diffusion of hydrogen peroxide across membranes. *J Biol Chem.* 2007;282:1183-1192.
34. Vergani L, Floreani M, Russell A, et al. Antioxidant defences and homeostasis of reactive oxygen species in different human mitochondrial DNA-depleted cell lines. *Eur J Biochem.* 2004;271:3646-3656.
35. Kuwahara Y, Roudkenar MH, Suzuki M, et al. The involvement of mitochondrial membrane potential in cross-resistance between radiation and docetaxel. *Int J Radiat Oncol Biol Phys.* 2016;96:556-565.
36. Lee JY, Jung GY, Heo HJ, et al. 4-Hydroxynonenal induces vascular smooth muscle cell apoptosis through mitochondrial generation of reactive oxygen species. *Toxicol Lett.* 2006;166:212-221.
37. Aikens J, Dix TA. Hydrodioxyl (perhydroxyl), peroxy, and hydroxyl radical-initiated lipid peroxidation of large unilamellar vesicles (liposomes): comparative and mechanistic studies. *Arch Biochem Biophys.* 1993;305:516-525.
38. Gaschler MM, Stockwell BR. Lipid peroxidation in cell death. *Biochem Biophys Res Commun.* 2017;482:419-425.
39. Zhang W, Zhong W, Sun Q, et al. Hepatic overproduction of 13-HODE due to ALOX15 upregulation contributes to alcohol-induced liver injury in mice. *Sci Rep.* 2017;7:8976.
40. Shintoku R, Takigawa Y, Yamada K, et al. Lipoxygenase-mediated generation of lipid peroxides enhances ferroptosis induced by erastin and RSL3. *Cancer Sci.* 2017;108:2187-2194.
41. Shah R, Shchepinov MS, Pratt DA. Resolving the role of lipoxygenases in the initiation and execution of ferroptosis. *ACS Cent Sci.* 2018;4:387-396.
42. Uchida K. HNE as an inducer of COX-2. *Free Radic Biol Med.* 2017;111:169-172.
43. Fang Q, Zhu Y, Wang Q, et al. Suppression of cyclooxygenase 2 increases chemosensitivity to sesamin through the Akt-PI3K signaling pathway in lung cancer cells. *Int J Mol Med.* 2019;43:507-516.
44. Ji GR, Yu NC, Xue X, et al. 4-Hydroxy-2-nonenal induces apoptosis by inhibiting AKT signaling in human osteosarcoma cells. *Sci World J.* 2014;2014:873525.
45. Schauen M, Spitkovsky D, Schubert J, et al. Respiratory chain deficiency slows down cell-cycle progression via reduced ROS generation and is associated with a reduction of p21CIP1/WAF1. *J Cell Physiol.* 2006;209:103-112.

SUPPORTING INFORMATION

Additional supporting information may be found online in the Supporting Information section at the end of the article.

How to cite this article: Tomita K, Takashi Y, Ouchi Y, et al. Lipid peroxidation increases hydrogen peroxide permeability leading to cell death in cancer cell lines that lack mtDNA. *Cancer Sci.* 2019;110:2856-2866. <https://doi.org/10.1111/cas.14132>